Supplementary Information

I. Theoretical Modeling of Absorption and Index of Refraction Spectra

When the conduction and valence bands of a semiconductor are populated by excited carriers, the complex dielectric function can change dramatically through many body effects, e.g. band filling. At a quasi-equilibrium state, such many body effects can be fully characterized, at least macroscopically, by two thermodynamically independent properties of carriers: density and temperature. A semi-phenomenological theoretical formalism proposed by Banyai and Koch accurately describes the optical properties of semiconductors over a wide range of temperatures and carrier densities in which the absorption $\alpha(\omega)$ is described by a generalized Elliot formalism [1-3]:

$$\alpha(\omega) \sim A(\omega) \sum_{\lambda} |\phi_{\lambda}(\boldsymbol{r}=0)|^2 \delta_{\Gamma}(\hbar\omega - E_{\lambda}) \qquad (1)$$

where $A(\omega) = \tanh\left(\frac{\beta}{2}\left(\hbar\omega - E_g - \mu\right)\right)$ is the band filling factor with $\beta = 1/k_B T_{eh}$, the total chemical potential is $\mu = \mu_e + \mu_h$, and the band gap is E_g. The temperature of EHP (T_{eh}) may be different from the lattice temperature. The band filling factor provides the correct cross over between absorption and gain: $A(\omega) < 0$ for $\hbar\omega < E_g + \mu$ results in negative absorption (gain) while $A(\omega) > 0$ for $\hbar\omega > E_g + \mu$ gives positive absorption. Band gap renormalization is included by considering a density dependent effective band gap. The wave function ϕ_{λ} in equation (1) was obtained by solving a modified Wannier equation where the Columb potential in Wannier equation is replaced by Yukawa potential (characterized by screening length of κ^{-1}). Thus, in this formalism relevant many body effects (band filling, band gap renormalization and plasma screening) have been included. By considering both bound states (excitons) and continuum states, the absorption spectrum reads[1]:

$$\alpha(\omega) \cong \frac{\bar{\varepsilon}}{c\sqrt{\varepsilon_0}} \tanh\left[\frac{\beta}{2}\left(\hbar\omega - E_g - \mu\right)\right] \Bigg\{ \sum_{l=1}^{[g^{1/2}]} \pi\delta_\Gamma\left(\frac{\hbar\omega - E_g}{E_R} + \left(\frac{1}{l} - \frac{l}{g}\right)^2\right)$$
$$\times \frac{2(g-l^2)(2l^2-g)}{l^3 g^2} \prod_{\substack{n=1 \\ n\neq l}}^{\infty} \frac{n^2[n^2l^2 - (g-l^2)^2]}{(n^2-l^2)(n^2l^2-g^2)}$$
$$+ \int_0^\infty dx\sqrt{x} \prod_{n=1}^{\infty}\left(1 + \frac{2gn^2 - g^2}{(n^2-g)^2 + n^2g^2x}\right)\delta_\Gamma\left(x - \frac{\hbar\omega - E_g}{E_R}\right)\Bigg\} \quad (2)$$

where c is the speed of light in vacuum, ε_0 is the material static dielectric constant, and $\bar{\varepsilon} = r_{cv}^2/2\pi a_0^3 E_R$ in which $a_0 = \hbar^2\varepsilon_0/me^2$ is the Bohr radius and $E_R = \hbar^2/2ma_0^2$ is the Rydberg energy with $m^{-1} = m_e^{-1} + m_h^{-1}$. The carrier density is related to the chemical potential and temperature through:

$$a_0^3 N_i = \frac{1}{2\pi^2}\left(\frac{m_i}{\beta m E_R}\right)^{3/2} \int_0^\infty dx\, x^{1/2} f(x - \beta\mu_i) \quad (3)$$

for $i = e, h$ and $f(x)$ is the Fermi distribution function. In equation (2), $E_g = E_{g0} + \delta E_g$ is the renormalized bandgap in which:

$$\delta E_g = E_R \times \begin{cases} -1 + \left(1 - \frac{1}{g}\right)^2 & for \quad g \geq 1 \\ -\frac{1}{g} & for \quad g < 1 \end{cases} \quad (4)$$

where $g = 12/\pi a_0 \kappa$ in which the inverse screening length κ reads:

$$(a_0\kappa)^2 = \frac{4}{\pi}\left(\frac{1}{\beta E_R}\right)^{1/2} \int_0^\infty dx\, x^{1/2} \sum_{i=e,h} \left(\frac{m_i}{m}\right)^{\frac{3}{2}} f(x - \beta\mu_i)\left(1 - f(x - \beta\mu_i)\right) \quad (5)$$

The delta function in equation 2 is defined as:

$$\delta_\Gamma(x) = \frac{E_R}{\pi\Gamma \cosh\left(\frac{E_R x}{\Gamma}\right)} \quad (6)$$

where Γ is a phenomenological broadening parameter. Combining the above relations, the absorption spectrum (equation 2) can be reduced to an expression which depends only on EHP density (N_{eh}) and temperature (T_{eh}) and intrinsic material parameters. The inversion of equation (3) allows one to calculate the chemical potentials $\mu_i(N_{eh}, T_{eh})$. Substituting the chemical potentials in equation (5), results in a

screening length and thus g which can be used in equation (4) to evaluate the renormalized band gap. Thus, all parameters in equation (2) are expressed as a function of density and temperature only.

Once the absorption spectrum is evaluated for each pair of density and temperature, the real part of the index of refraction can be computed by applying the Kramers-Kronig relation:

$$n(\omega, N_{eh}, T_{eh}) = \frac{c}{\pi} P \int_0^{\infty} d\omega' \frac{\alpha(\omega', N_{eh}, T_{eh})}{\omega'^2 - \omega^2} \tag{7}$$

Thus, the complex index of refraction reads:

$$\boldsymbol{n}(E, N_{eh}, T_{eh}) = \frac{\hbar c}{\pi} P \int_0^{\infty} dE' \frac{\alpha(E', N_{eh}, T_{eh})}{E'^2 - E^2} + \frac{i\hbar c}{E} \alpha(E, N_{eh}, T_{eh}) \tag{8}$$

For material parameters we used $m_e = 0.0665\, m_0$, $m_h = 0.52\, m_0$, $\varepsilon_0 = 12.35$, $a_0 = 1.243 \times 10^{-6}\, cm$, $E_R = 4.2\, eV$, $E_{g0} = 1.519\, eV$, and $\Gamma = 4\, meV$ consistent with FWHM of photoluminescence at low density.

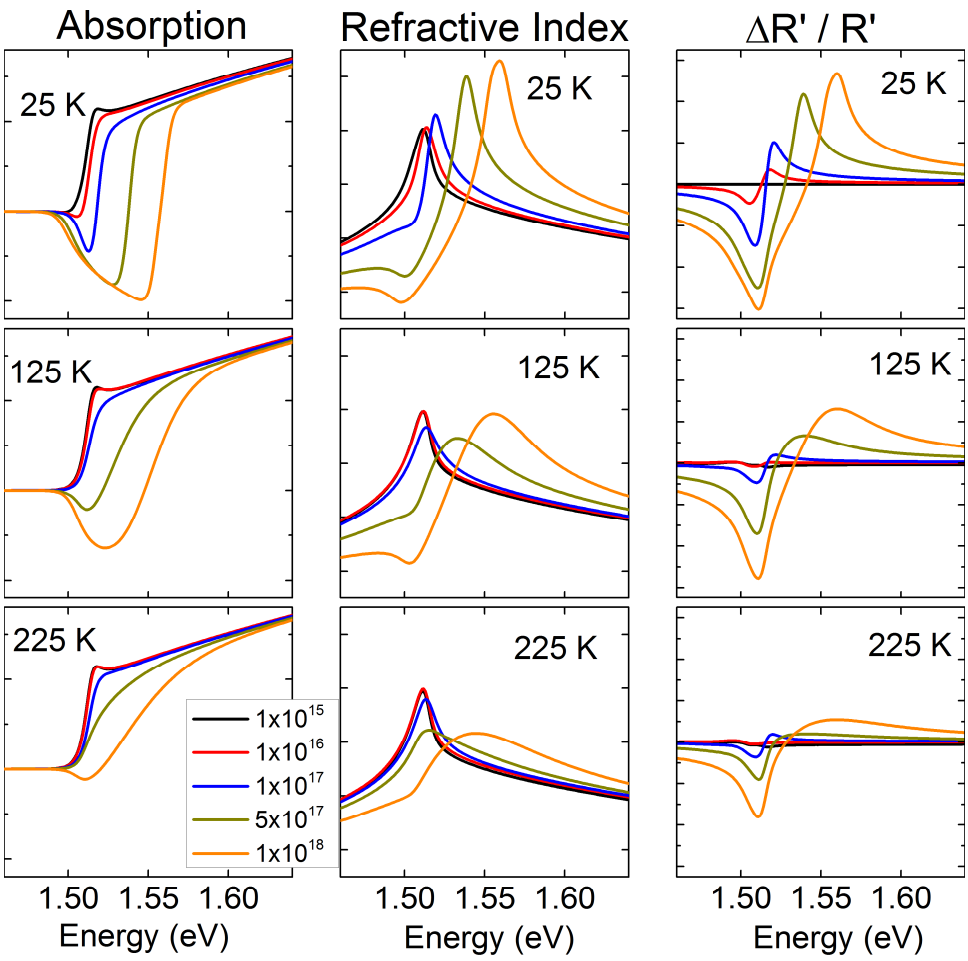

Figure **1**: Comparison of calculated absorption (left column) and refractive index (middle column) and change in Rayleigh spectrum of a nanowire with 150 nm diameter (right column) for various densities ($\boldsymbol{N_{eh}}$) and temperatures ($\boldsymbol{T_{eh}}$) of the electron-hole plasma. The changes in the Rayleigh spectrum are calculated with respect to the spectrum with $\boldsymbol{N_{eh} = 10^{15}\ cm^{-3}}$ and $\boldsymbol{T_{eh} = 25\ K}$.

Figure 1 compares the calculated absorption and refractive index for various densities and temperature using above expressions. In the absorption spectra, at low densities the exciton resonance is shown by a small peak at the right side of the absorption edge. By increasing the density, eventually the exciton resonance diminishes due to the Mott transition. By increasing the density further, band filling becomes important and a region with negative absorption (gain) appears. An increase in the temperature results in an increase in the Mott density and the density of the absorption/gain cross over. The middle column in Figure 1 shows the refractive index calculated by applying the Kramers-Kronig relation to the absorption spectrum. The right column shows the change in the Rayleigh spectrum of a nanowire with 150 nm diameter where the background density and temperature was taken at $N_{eh} = 10^{15}\ cm^{-3}$ and $T_{eh} = 25\ K$. As demonstrated in Figure 1, the band filling, band gap renormalization and plasma screening (which can be seen easily in absorption spectra) does not map simply to the change of the Rayleigh spectrum. Thus

the inverse problem of determining the many body effects from the Rayleigh spectrum requires a fitting procedure.

II. Data Fitting Procedure

The chi-squared was defined for a two dimensional map as following:

$$\chi^2 = \sum_i \sum_j \left(\frac{\Delta R'}{R'}(t_i, E_j) - y_i - A_i e^{i\theta} \left(\boldsymbol{n}\left(E_j, N_{eh}(t_i), T_{eh}(t_i)\right) - \boldsymbol{n}(E_j, N_0, T_0) \right) \right)^2 \qquad (9)$$

where $\frac{\Delta R'}{R'}(t_i, E_j)$ is the experimentally measured transient Rayleigh scattering signal at energy E_j and time t_i after initial excitation. The parameters θ (modulation phase) and N_0 and T_0 (background density and temperature) do not depend on time or energy. y_i's and A_i's are the background signal and signal amplitude which do not depend on the energy but may vary slightly in time due to other possible effects not included in theory such as dependency of optical transition dipole coupling on density and temperature. To measure the modulation phase, background density and temperature, and time-dependent density and temperature the chi-squared defined by equation (9) was minimized numerically. The quality and sensitivity of this procedure is demonstrated in Figures 2 and 3 for times at 6 ps and 100 ps. Such comparisons were made by varying the density by 15% around the fit value while the temperature was fixed (left panel) and similarly, a 15% variation of the temperature at fixed density at the fit value. This comparison at both 6 ps and 100 ps after excitation (bottom graphs in Figure 2 and 3), suggest that the fitting procedure is somewhat more sensitive to the EHP density than to the temperature.

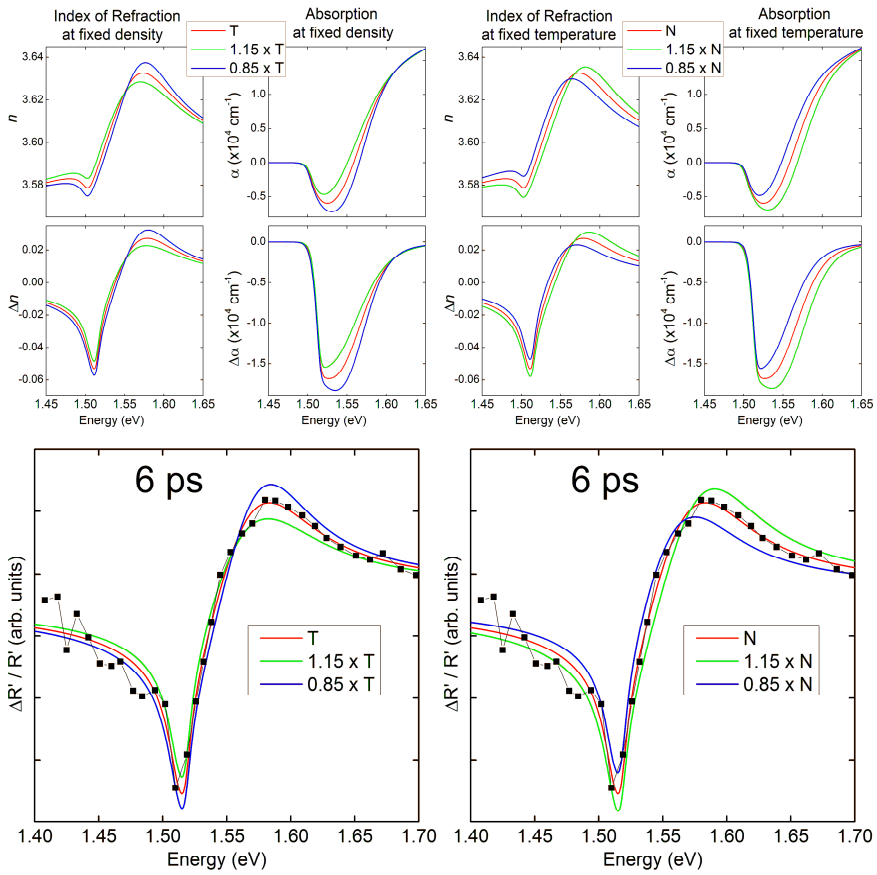

Figure **2**: Comparison of the fits with different values for density and temperature at 6 ps after excitation. The solid red spectrum is calculated for the fit values of density and temperature at $1.67 \times 10^{18}\ cm^{-3}$ and 201 K respectively. The left panel compares the absorption and the index of refraction spectra resulted from the fit procedure (red line) with the spectra obtained by $\pm\mathbf{15}\%$ variation of temperature while the density is kept fixed (blue and green lines). Similarly, the right panel compares the fit results with $\pm\mathbf{15}\%$ variation in density while the temperature is kept fixed. At the bottom, the filled boxes are the experimental values and the interconnecting black lines are guides for the eye.

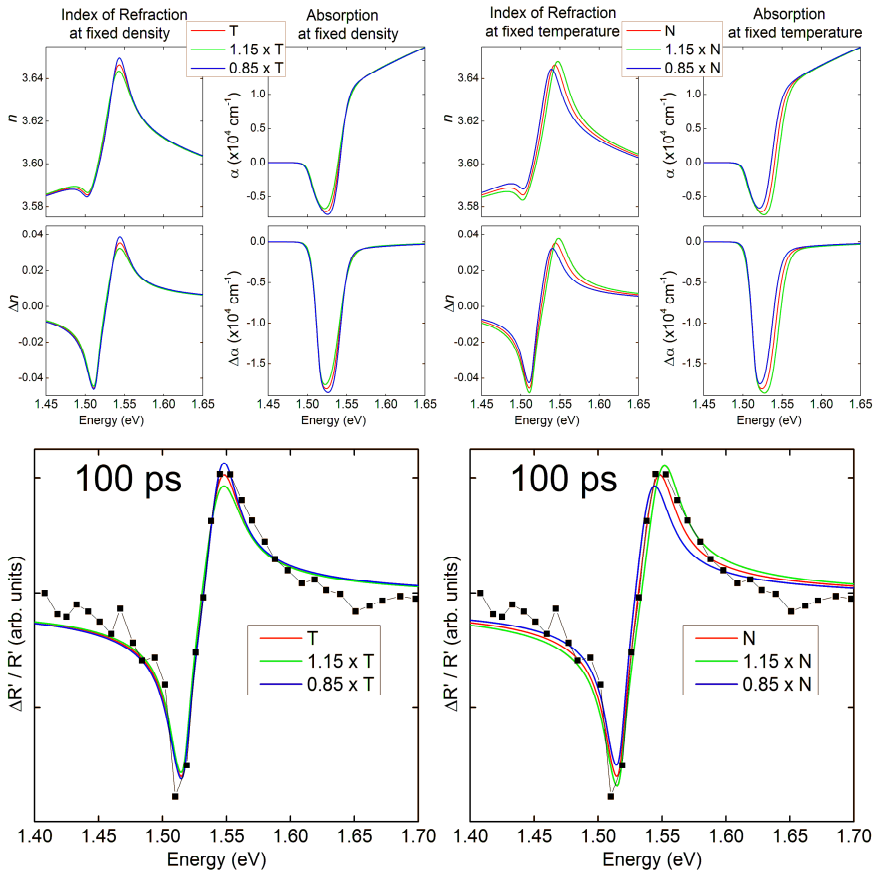

Figure **3:** Comparison of the fits with different values for density and temperature at 100 ps after excitation. The solid red spectrum is calculated for the fit values of density and temperature at $6.02 \times 10^{17}\ cm^{-3}$ and $63\ K$ respectively. The left panel compares the absorption and the index of refraction spectra resulted from the fit procedure (red line) with the spectra obtained by a $\pm\mathbf{15}\%$ variation of temperature while the density is kept fixed (blue and green lines). Similarly, the right panel compares the fit results with a $\pm\mathbf{15}\%$ variation in density while the temperature is kept fixed. At the bottom, the filled boxes are the experimental values and the interconnecting black lines are guides for the eye.

III. Carrier dynamics

To analyze the measured EHP density, we consider a finite nanowire with length L which extends from $-L/2$ to $L/2$. Including one dimensional ambipolar diffusion and linear and bimolecular recombination, the rate equation governing the carrier dynamics reads:

$$\frac{\partial N_{eh}(x,t)}{\partial t} = G + D_a \frac{\partial^2 N_{eh}(x,t)}{\partial x^2} - \frac{N_{eh}(x,t)}{\tau} - B N_{eh}(x,t)^2 \qquad (10)$$

Where G is the generation term associated with the intensity and size of the pump beam which was focused at the center of the nanowire. The intensity of the pump beam has a Gaussian profile with FWHM of $2\sqrt{log\ 2}$. Since the pump pulse width (~250 fs) is much smaller than the relevant time scale in describing the dynamics, the amplitude of the Gaussian is determined by the number of carriers injected into a nanowire of finite length. Also, the surface recombination at either ends of the nanowire resulted in the boundary conditions:

$$\left(\frac{\partial N_{eh}(x,t)}{\partial x}\right)_{x=\pm L/2} = -\frac{S_0}{D_a} N_{eh}(x = \pm L/2\,, t) \qquad (11)$$

where S_0 is the surface velocity. Then Equation (10) at $x = 0$ ($\sim\langle N_{eh}\rangle_{probe}$) is fitted to the measured EHP density. In the fit the surface velocity $S_0 = 10^5 cm/s$ and the length of the nanowire at $L = 3.2$ micron (measured from TEM images) were kept fixed while the free parameters include ambipolar diffusion D_a, linear recombination constant τ, bimolecular recombination constant B, initial density and pump Gaussian width w. The Gaussian width of the pump (w) was measured at 0.8 microns and is consistent with the optical image of the pump laser spot.

IV. Energy loss rate *equation*

The total energy loss rate due to emission of LO and acoustic phonons may be written:

$$\langle\frac{dE}{dt}\rangle = c\,\langle\frac{\partial E}{\partial t}\rangle_{LO} + \langle\frac{\partial E}{\partial t}\rangle_{AC} \qquad (12)$$

where the left hand side is the total energy loss rate of the EHP and the terms in the right hand side correspond to energy loss rate due to emission of LO and acoustic phonons respectively. On the right side, the factor c accounts for re-absorption of LO phonons due to high occupation of phonon's state at early times (see the text). The averaging is over a Fermi distribution of EHP associated with the density and temperature of $N_{eh}(t)$ and $T_{eh}(t)$. The left hand side can thus be written as:

$$\langle\frac{dE}{dt}\rangle = \frac{3}{2}\left(\sum_{i=e,h} \frac{F_{3/2}(\mu_i/k_B T_{eh})}{F_{1/2}(\mu_i/k_B T_{eh})}\right)\frac{dT_{eh}}{dt} \qquad (13)$$

where the Fermi integrals (F_j) are treated as constant in time. The Fermi averaged LO phonon emission rate by carriers (Frohlich coupling) reads[4, 5]:

$$\langle\frac{\partial E}{\partial t}\rangle_{LO} = \sum_{i=e,h} \frac{e^2 m_i^2 k_B T_{eh}}{K\,\hbar^5\pi^2 N_{eh}}\left(\frac{1}{\varepsilon_\infty}-\frac{1}{\varepsilon_0}\right)\left(N_{LO}(T_{eh})-N_{LO}(T_l)\right)\int_0^\infty dq\,\frac{(\hbar\omega_{LO})^2}{q}$$
$$\times Ln\left[\frac{1+\exp[(-\hbar^2/8m_i k_B T_{eh})(q-2m_i\omega_{LO}/\hbar q)^2+\mu_i/k_B T_{eh}]}{1+\exp[(-\hbar^2/8m_i k_B T_{eh})(q+2m_i\omega_{LO}/\hbar q)^2+\mu_i/k_B T_{eh}]}\right] \quad (14)$$

where N_{eh} and T_{eh} are the density and temperature of EHP, T_l is the lattice temperature, ε_0 and ε_∞ are material static and high frequency dielectric constants, and $\hbar\omega_{LO}$ is the energy of LO phonons. The factor K is equal to 1 for electrons and 2 for holes[4, 5]. Also, $N_q(T) = \left(\exp\left(\hbar\omega_q/k_B T\right)-1\right)^{-1}$ is the phonon occupation number. Similarly, the Fermi average of the emission rate of acoustic phonons, described by the acoustic phonon deformation potential (E_{AC}), reads:

$$\langle\frac{\partial E}{\partial t}\rangle_{AC} = \sum_{i=e,h} \frac{m_i^2 E_{AC}^2 k_B T_{eh}}{4\pi^3\,\hbar^3\rho N_{eh}}\int_0^\infty dq\; q^3\left(N_q(T_{eh})-N_q(T_l)\right)$$
$$\times Ln\left[\frac{1+\exp[(-\hbar^2/8m_i k_B T_{eh})(q-2m_i v_s/\hbar)^2+\mu_i/k_B T_{eh}]}{1+\exp[(-\hbar^2/8m_i k_B T_{eh})(q+2m_i v_s/\hbar)^2+\mu_i/k_B T_{eh}]}\right] \quad (15)$$

Where v_s is the sound velocity, ρ is the mass density of the material, and $\hbar\omega_q \approx \hbar q v_s$ is the energy of an acoustic phonon with wave vector q.

Combining equations (12)-(15) results in the energy loss rate equation that we have used to numerically fit the measured time-dependent EHP temperature. The only free parameters are the factor c and acoustic phonon deformation potential E_{AC}. The other parameters are kept fixed: $\hbar\omega_{LO} = 35\ meV$, $v_s = 3.57 \times 10^5 cm/s$, $\rho = 5.81\ g/cm^{-3}$, $\varepsilon_\infty = 10.94$, $\varepsilon_0 = 12.35$, $m_e = 0.0667\ m_0$ and $m_h = 0.52\ m_0$. Note that density N_{eh} and chemical potentials μ_i, which appear explicitly in the energy loss rate equation (equations 12-15), are time-dependent. These are incorporated directly into the equation using the measured time-dependent values from the fits to the transient Rayleigh spectra. Once the factor c and the acoustic phonon deformation potential E_{AC} are determined, the energy loss rate due to emission of LO and acoustic phonons are evaluated using equations (14) and (15).

V. References

1. Banyai, L.; Koch, S. W. *Zeitschrift Fur Physik B-Condensed Matter* **1986,** 63, 283-291.

2. Haug, H.; Koch, S. W. *Quantum Theory of the Optical and Electronic Properties of Semiconductors;* World Scientific Publishing Co: Singapore, 2004; .

3. Lee, Y. H.; Chavezpirson, A.; Koch, S. W.; Gibbs, H. M.; Park, S. H.; Morhange, J.; Jeffery, A.; Peyghambarian, N.; Banyai, L.; Gossard, A. C.; Wiegmann, W. *Phys. Rev. Lett.* **1986,** 57, 2446-2449.

4. Prabhu, S. S.; Vengurlekar, A. S.; Roy, S. K.; Shah, J. *Physical Review B* **1995,** 51, 14233-14246.

5. Leo, K.; Ruhle, W. W.; Ploog, K. *Physical Review B* **1988,** 38, 1947-1957.